ULTRACOLD ATOMS FOR ULTRASTABLE FREQUENCY STANDARDS*

K. Szymaniec, W. Chałupczak, S.N. Lea, and D. Henderson

National Physical Laboratory
Queens Road, Teddington, Middlesex, TW11 0LW, UK

(Received June 3, 2002)

In recent years, the application of laser cooling has led to significant advances in atomic frequency standards. In particular, the caesium fountain has advanced the accuracy of the realisation of the SI second by about an order of magnitude, to 1 in 10^{15}. It is anticipated that optical frequency standards, either single trapped ions or cold neutral atoms, will provide advances in frequency stability. Highly stable optical frequencies will be translated to microwave frequencies by a revolutionary new technique. This paper gives a brief review of current techniques in frequency metrology. The atomic physics processes underlying the progress, as well as those responsible for the limitations to the performance of these new standards, are discussed.

PACS numbers: 06.20.Fn, 32.80.Pj

1. Introduction

Laser cooling and trapping of atoms and ions has been one of the most dynamic areas of research in physics in recent years. This has been recognised by the award of the Nobel Prize for Physics, in this field, in 1989, 1997 and in 2001. The achievement of Bose–Einstein condensation is the most noteworthy recent result of this activity. Tools for manipulating cold atoms, developed over this period, are now used routinely in many laboratories for a variety of studies of fundamental processes in atomic physics. The most significant application remains in metrology, where cold atoms have enabled an order-of-magnitude improvement in the accuracy and stability of the caesium primary standard of time and frequency.

There have been several reviews of research achievements in the area of frequency standards in recent years [1–3]. It is beyond the scope of this paper to cover the enormous range of work in this field. The brief review,

* Presented at the Photons, Atoms and All That, PAAT 2002 Conference, Cracow Poland, May 31–June 1, 2002.

given here, pays particular attention to cold atom microwave standards, to advances in laser cooling of neutral atoms and to the latest achievements in metrology at optical frequencies. The paper provides an overview of the ways in which advances in laser cooling have spawned related advances in frequency metrology.

Section 2 recalls the operation of the thermal beam caesium standard and identifies the principal limitations to its accuracy and stability. Section 3 discusses the ways in which the instability and the systematic shifts are reduced in the laser-cooled caesium standard (the caesium fountain). Section 4 discusses the remaining, dominant, systematic shift due to collisions between the cold atoms and explains how improvements might be obtained by the use of still colder atoms. Some methods for cooling further are explained in Section 5 and the ultimate limit to the stability of a caesium standard is examined in Section 6. In Section 7 the promise of optical frequency standards, to provide orders of magnitude advances in accuracy and stability, is discussed. A brief review is presented of the research effort into the development of frequency standards based on optical transitions in laser-cooled atoms and ions, being carried out by national standards laboratories such as NPL. The difficulty of performing comparisons between optical and microwave with the necessary level of precision is introduced as the major impediment to the use of optical frequency standards. The recent development of optical frequency combs based on mode-locked femtosecond lasers is a significant advance, linking optical and microwave.

2. Thermal beam atomic frequency standards

Modern day atomic clocks have their roots in the molecular beam resonance experiment devised by Rabi in 1930s [4]. A flux of atoms exits an oven and passes the state-selection A-magnet, where an inhomogeneous magnetic field separates atoms with different magnetic moments (Fig. 1). The atoms pass through an oscillating radio-frequency (rf) magnetic field in a region of uniform static magnetic field (the C-region). The atoms then pass through a further state-selecting B-magnet and on to a detector, arranged to be sensitive to a sub-set of atom trajectories. The trajectory depends on the magnetic moment of the atom as it passes the A and B magnets. The frequency of the rf field is adjusted so as to cause a change of magnetic moment, as evidenced by a change in the flux reaching the detector.

The idea of the apparatus forming a frequency standard is also attributed to Rabi [5]. An rf Local Oscillator (LO) is stabilized by means of frequency modulation to a narrow atomic or molecular resonance in the GHz range. The precision in determining the resonant frequency in this apparatus is limited by the interaction time between the atoms and the rf field (transit

time through the cavity). This time is constrained by the need to use a resonant cavity of dimension on the order of the wavelength of the rf radiation ($\sim$ 3 cm) and by the thermal velocities of the atomic beam. For a caesium beam leaving an oven at 360 K, the most probable velocity is 290 m/s, yielding an interaction time of about 100 μs, hence a resonance width of 10 kHz. In longer cavities, the rf field contains a travelling wave component to an increasing extent. This causes a first order Doppler shift in the resonance.

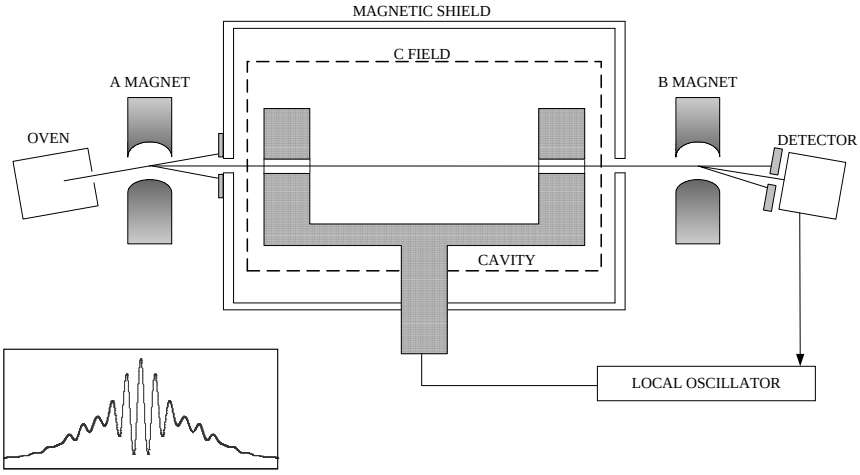

Fig. 1. Generic scheme of a caesium beam frequency standard with the Ramsey-type interrogation. The U-shaped Ramsey cavity is driven from an oscillator, which is servoed so as to maintain the flux on the detector. Insert: Ramsey fringes typically observed in a thermal beam standard.

In order to overcome these dimensional constraints, the separated oscillatory fields method was introduced by Ramsey [6]. A microwave cavity, in the shape of a "U", is fed from the centre (Fig. 1). The rf interaction occurs at two places between the state selection magnets. The spacing of these interactions is no longer limited by the rf wavelength and can be up to several metres, enabling the linewidth to be reduced by some two orders. An rf field with amplitude corresponding to a $\pi/2$ pulse prepares the atoms in a coherent superposition of two states during the first passage through the cavity and then probes the evolution of the atomic coherence during the second passage. The fringes are the result of interference between the freely evolving atomic coherence and the oscillating field. The observed line shape (the well known Ramsey fringes) is the Fourier transform of the temporal shape of the two-pulsed interaction. The frequency of the central fringe is the output of the measurement (see insert in Fig. 1).

Work towards a laboratory frequency standard based on a molecular atomic beam began in the National Bureau of Standards (the present-day NIST) in the USA in the 1950s [7]. The first caesium beam apparatus to be operated on a regular basis was constructed by Essen and Parry at the National Physical Laboratory (NPL) in Great Britain [8]. Their work, in conjunction with the United States Naval Observatory (USNO) [9], measuring the caesium transition with respect to the Ephemeris second, led the International Conference on Weights and Measures (CIPM) to redefine the second from an astronomical definition to a quantum based standard: since 1967 the second has been defined as the duration of 9 192 631 770 periods of the radiation corresponding to the transition between the two hyperfine levels of the ground state of the caesium-133 atom. Caesium beam frequency standards have been constructed in many laboratories perhaps the most notable being a series of standards operated continuously over a period of years at Physikalisch-Technische Bundesanstalt (PTB) in Germany [10].

A primary frequency standard is an apparatus constructed to realise the SI second. The accuracy of a primary standard is the extent by which the value obtained from the measurement may deviate from the true value (the second or hertz in this case), with a particular level of confidence. In order to establish the accuracy, it is necessary to quantify (by measurement or calculation) all the possible systematic effects that may shift the measured frequency together with the uncertainties in these. The ability to quantify the frequency shifts distinguishes a primary standard from other, usually commercially produced, caesium beam devices.

The random uncertainty, or stability, of the primary frequency standard also contributes to the total uncertainty of the realisation. The stability is usually quantified by means of the Allan deviation [11]. For caesium beam devices dominated by white noise the Allan deviation, $\sigma_y(\tau)$, decreases with the inverse square root of the measurement time, τ:

$$\sigma_y(\tau) = \left[\pi Q \left(\frac{S}{N}\right)\right]^{-1} \left(\frac{1}{\tau}\right)^{1/2}, \tag{1}$$

where the line Q factor is defined as $Q = \nu/\delta\nu$; $\delta\nu$ being the width of the central Ramsey fringe, ν the resonance frequency and S/N the signal to noise ratio.

Many of the systematic shifts are quantified by perturbing the relevant operating parameter and measuring the change in frequency against a stable reference. Thus the accurate estimation of systematic uncertainties requires that the stability is adequate for manageable averaging times. It is necessary to operate primary frequency standards only long enough to make a measurement and establish an uncertainty budget. Other devices, such as hydrogen masers, are often better suited to continuous operation as clocks.

Having corrected the measured value for the systematic shifts, the systematic and random uncertainties (stability) can be combined to give the standard's accuracy with a given confidence.

Having been developed over some 50 years, caesium beam primary standards are now quite mature. Many sources of systematic frequency shifts have been identified. Several of these can be reduced such that their contribution to the uncertainty is insignificant to the extent that a correction need not be applied. We will now highlight the shifts that substantially contribute to the uncertainty budget.

2.1. Quadratic Zeeman

The linear Zeeman effect is eliminated by the use of atoms in the $m_F = 0$ Zeeman sublevel. However, the C-field applied to lift the degeneracy of the magnetic sublevels causes a second-order Zeeman shift of the $m_F = 0$ atoms. Transitions between magnetically sensitive sublevels ($m_F \neq 0$) can be used to determine the magnitude of the C-field. The second order shift can then be calculated.

2.2. Quadratic Doppler

The quadratic Doppler shift is due to the velocity of the atoms relative to the reference frame in which the rf field is generated. For beam devices, with beam velocities of 100 m/s to 250 m/s, the relative shift is -5×10^{-14} to -3×10^{-13}. The shift is calculated from an estimate of the velocity distribution of the atoms in the beam, together with the variation of the transition probability with the microwave interaction time.

2.3. Cavity phase

The Cavity phase shift occurs because the phase of the radiation in the two arms of a Ramsey cavity cannot be exactly equal, due to manufacturing tolerances in the lengths and losses in the waveguide. The result is a phase difference between the centre of the apertures in the two cavities. This gives a frequency shift,

$$\Delta\nu = \frac{\Phi_1 - \Phi_2}{2\pi T},$$

where Φ_1 and Φ_2 are the phases at the two apertures and T the time of flight between the arms. Primary standards are constructed with a caesium source at each end, to permit reversal of the beam direction. The cavity phase shift is identified as one half of the resulting frequency change, by assuming that the shift is symmetric. However the phase also varies across

the cavity aperture (distributed phase shift) so that $\Delta\nu$ varies with atom trajectory. Thus the effectiveness of the beam reversal is dependant on the geometric accuracy of the process.

2.4. Detuning of the μ-wave cavity

The rf oscillator is servoed, on average, to the line centre, ν_0, by frequency modulation (deviation $\Delta\nu_m$) and synchronous detection of the error signal. Typically, the frequency is square-wave modulated to the 50% transition probabilities found on the two sides of the central Ramsey fringe. The Ramsey cavity is resonant at a frequency near, but not equal to ν_0. Thus, for a given rf power applied to the cavity, the field amplitude will differ at $\nu_0 - \Delta\nu_m$compared with$\nu_0 + \Delta\nu_m$. It follows that the 50% transition probabilities are not found for equal detuning from the true line centre, and that ν_0 is shifted to an extent depending on the cavity resonance detuning and Q-factors of both the cavity and atomic transition.

2.5. Asymmetry of Zeeman population

The flux of atoms reaching the detector in the $m_f = 0$ sublevel will be overlapped by the edges of the beam of atoms in the $m_f = \pm 1$ Zeeman sublevelsΔ to an extent depending on the applied C field. The flux of these atoms in $m_f = +1$ and $m_f = -1$ will differ as they have different effective magnetic moments in the state selecting fields. Thus the servo maximising the beam flux will be skewed to an extent depending on the asymmetry and give a frequency shift.

2.6. AC Stark (thermal radiation)

The blackbody radiation gives rise to an AC Stark shift and can be estimated from the measured DC Stark shift and the mean square value of the AC field. The limitation to the corresponding uncertainty is in estimating the mean square value of the AC field due to uncertainty in the temperature of the vacuum vessel and the emissivities of the materials. The frequency is shifted by approximately 2×10^{-16} for a temperature change of 1 K at 298 K [12].

2.7. AC Stark (fluorescence)

An AC Stark shift is present in some thermal beam frequency standards, in which the state preparation is done by optical pumping instead of magnetic selection as in the original apparatus of Rabi and Ramsey. This method offers the advantage of a higher flux of atoms contributing the signal, and hence better stability. Also, in the absence of the strong selecting magnets,

the design of the magnetic shields, necessary to assure the uniformity of the C-filed, is simplified. However, the AC Stark shift due to fluorescence from the atomic beam at the preparation and detection positions is a difficulty [13, 14].

3. Cold atomic fountains

The major factor limiting the accuracy of thermal beam frequency standards is the cavity phase difference. This can be completely removed in a fountain where atoms, launched vertically, are turned back by gravity and hence can be made to pass twice through a single microwave cavity. The original idea of a fountain, using slow atoms from the low velocity tail of the Maxwell–Boltzmann distribution, came from Zacharias in the 1950s. The experiment was unsuccessful because there are very few slow atoms in the thermal beam, compared to the Maxwell–Boltzmann distribution, due to collisions with faster atoms. Only in the 1990s, with the development of laser cooling and trapping of neutral atoms [15], has it been possible to implement the fountain configuration successfully for precision spectroscopy and atomic frequency standards. The use of slow atoms has substantially reduced several other systematic frequency shifts. Slow atoms also allow longer interaction times, giving a line-Q factor of 10^{10} and improved stability.

The first cold atomic fountain was demonstrated by Chu and co-workers in 1989 [16]. A cloud of 5×10^7 sodium atoms was collected and cooled in a magneto-optical trap (MOT) and then pushed upwards by a radiation pressure pulse. At their apogee the atoms were exposed to two microwave pulses constituting a Ramsey-type interrogation. The 2 Hz width of the observed fringes demonstrated the potential of spectroscopic methods using laser cooled atoms. However, a significant drawback of this pioneering experiment was the launching technique. A simple radiation pressure pulse, due to the random character of the photon scattering process, causes additional heating and thermal expansion of the atomic cloud, resulting in a reduced number of detected atoms and, consequently, a poor signal-to-noise ratio. Experiments in Paris and in Stanford [17, 18] introduced the so-called moving molasses, which provides a much more efficient launching mechanism. The optical molasses is created by three mutually orthogonal pairs of counter-propagating laser beams which damp the atomic motion. If one pair of beams is directed vertically, it is possible to create a frame moving with velocity $v_0 = \lambda \Delta f$ by shifting the frequency of the down-going beam by $-\Delta f$ and that of the up-going by $+\Delta f$. The atoms are swiftly accelerated and then cooled. The cooling light is switched off, before the atoms move out of the intersection region of the beams, leaving them to continue their free flight under gravity with the initial velocity v_0.

The Paris experiment used caesium atoms and has formed the basis for all the fountain clock experiments being developed in various metrology laboratories worldwide [19–26]. A typical fountain apparatus, as shown in figure 2, consists of three parts: *(i)* the magneto-optical trap (MOT) or molasses region, *(ii)* the free flight and microwave interaction tube and *(iii)* the detection region. The MOT is loaded from a caesium vapour at a pressure of 10^{-8} mbar. The pressure in region *(ii)* and *(iii)* is kept below 10^{-9} mbar to minimise collisions of cold atoms with the background gas. The MOT is used solely as an efficient source of cold atoms. The atoms in the MOT are strongly perturbed by light, static magnetic field and collisions and therefore

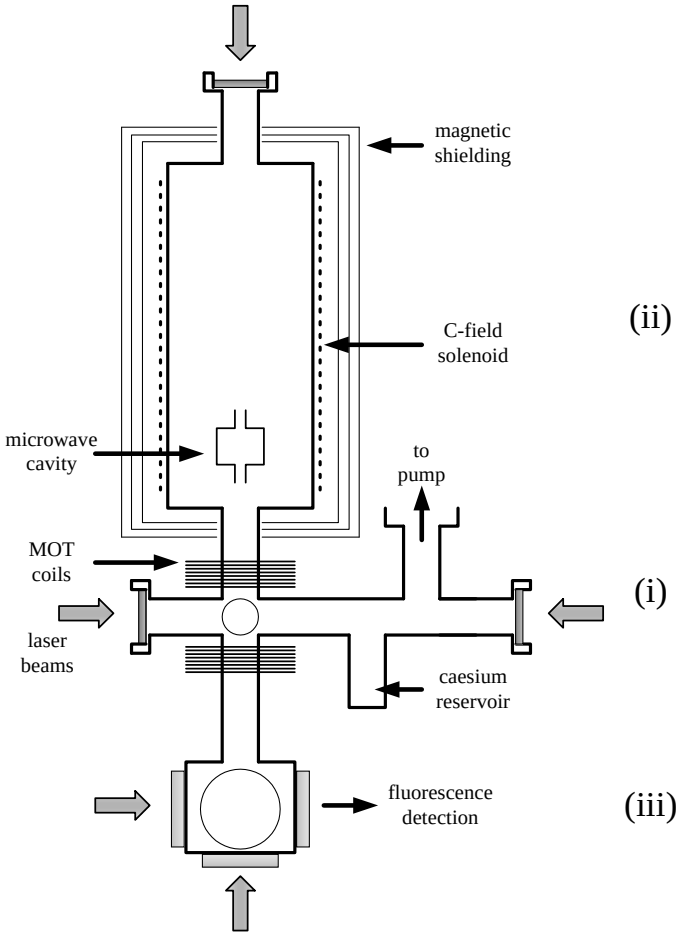

Fig. 2. Schematic diagram of the laser cooled caesium fountain at NPL. The regions *(i)–(iii)* as well as the operation cycle are described in the text.

cannot be used for precision spectroscopy. The number of atoms returning back to the detection region has to be maximised in order to achieve a satisfactory S/N ratio. Efficient loading of the MOT is required, together with cooling the launched atoms to a low temperature. However, the two aims are achieved for two different sets of parameters in laser intensity, detuning and magnetic field. Thus, if the parameters are to be optimised, it is only feasible for the fountain to operate in a sequential, or pulsed mode. A typical sequence consists of loading the trap, launching, cooling in the moving molasses, free flight through the Ramsey interaction zone, and detection. The sequential operation has the further advantage of reducing the AC Stark shift due to fluorescence from the trap or the background Cs vapour. Having passed through the microwave cavity for the second time, the atoms are detected by means of laser-induced fluorescence.

Ramsey fringes obtained with the NPL fountain are shown in figure 3a. The central fringe (Fig. 3(b)) has a full width at half maximum ($\Delta\nu$) of 1.0 Hz in the case of atoms reaching 30 cm above the centre of the microwave cavity. It is impractical to build a higher fountain in order to achieve significantly narrower fringes, as the fringe width is inversely proportional to the square root of the fountain height. High stability, or low statistical uncertainty in determining the centre of the fringe, can be achieved by high S/N or long averaging times. As in thermal beam frequency standards, the fountain standard locks the LO that drives the microwave cavity to the central Ramsey fringe. Every fountain cycle the LO frequency is toggled to $\nu_{\mathrm{Cs}} - \Delta\nu/2$ or $\nu_{\mathrm{Cs}} + \Delta\nu/2$, where the fountain signal is most sensitive to LO frequency changes. The fountain signal is measured then ν_{Cs} is calculated and used to steer the LO.

The fractional frequency stability of the first LPTF fountain in Paris, calculated from the S/N ratio, was 3×10^{-12} in 1s, which was comparable to the best thermal beam standards at that time. In the 1990s many improvements to fountain technology have been introduced aiming to achieve better stability and accuracy [27].

The major limitation of the S/N and hence the stability of the early fountains was the fluctuations, usually 2–5%, of the total number of caesium atoms detected, N_{at}. A *double detection* scheme was devised to address the problem. The atoms fall through two sets of retro-reflected laser beams, tuned closely to the cycling transition normally used for cooling. While passing across the detection beam, caesium atoms in the $F = 4$ sublevel of the ground state each scatter around 10^4 photons, which are typically collected with 1% efficiency. The retro-reflected beam of the upper set is blocked in its lower part. This removes the detected $F = 4$ atoms by radiation pressure. The lower detection beam is combined with a repumping beam, allowing the atoms in $F = 3$ (lower sublevel) to be detected in the same way as were the

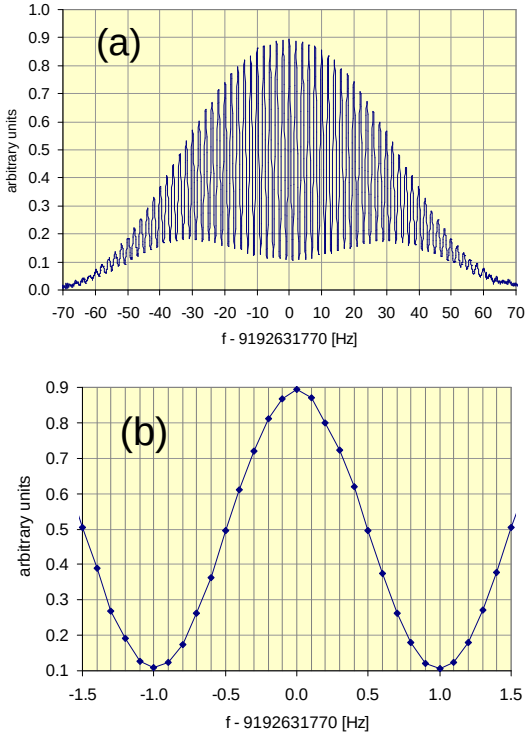

Fig. 3. (a) — Ramsey fringes observed in the NPL fountain. Large number of visible fringes is a consequence of the narrow velocity distribution of the laser cooled atoms. (b) — Central fringe (FWHM = 1 Hz) used to stabilise the local oscillator.

$F = 4$ atoms in the upper beam. The detection signal acquired can thus be normalized to N_{at}. Further improvements have been made by using lower noise detectors and amplifiers to measure the fluorescence, further narrowing of the linewidth of the detection laser, and stabilising its intensity. In some designs, higher collection efficiency (up to 20–30%) has been achieved by increasing the effective solid angle of the detection [21]. Such improved fountains have reached S/N levels of several 10^2 up to 10^3.

The technical noise of the detection having been significantly reduced, other more subtle effects become significant, such as the noise of the LO and the quantum projection noise. There is a significant effect on the stability due to the sequential operation. For that proportion of the operating cycle during which there is no atomic coherence (the *dead time*), there is no information about the behaviour of the LO. The LO acts as a "fly-wheel" oscillator during this dead time. As a consequence, any phase slips of the

LO occurring during the dead time which are synchronized with the fountain cycle time, T_c, cannot be corrected for. In other words, Fourier components of the LO phase noise close to integral multiples of $1/T_c$ are down-converted to the narrow bandwidth of the LO noise $(1/\tau)$ achieved after long averaging times ($\tau \gg T_c$) [28]. State-of-the-art quartz oscillators, commonly used as LO in fountain experiments, limit the stability to 1–2 $\times 10^{-13}\tau^{-1/2}$.

An improved stability, $4 \times 10^{-14}\tau^{-1/2}$, has been achieved by using a cryogenically cooled sapphire oscillator as the LO [29]. Utilising the spectral purity of the sapphire oscillator, it was possible to demonstrate the fundamental limit of the atomic fountain stability, that of Quantum Projection Noise (QPN). During the first Ramsey interaction the atoms are prepared in a coherent superposition of the two sublevels of the ground state ($F = 3$ and $F = 4$). During the second Ramsey interaction this superposition is *projected* onto one or the other sublevel. The noise of detecting *e.g.* $F = 3$ atoms can be calculated by Poisson statistics as, $\sigma_{F=3} = \sqrt{N_{\rm at}\, p\,(1-p)}$ where p is the probability of detecting the atom in a given state. Quantum projection noise cannot be removed by the normalization procedure described above. As the fountain normally operates at frequencies detuned from the centre of the atomic resonance by half a fringe width, where $p = 1/2$, the QPN is at a maximum. For the case of 10^5 atoms detected every cycle in the experiment of Ref. [29] the QPN dominated and limited the fountain stability to $6 \times 10^{-14}\tau^{-1/2}$. The QPN can be reduced by increasing the number of detected atoms. However, the increased rate of collision between the cold atoms at the higher atom density will then limit the fountain's accuracy.

TABLE I

Major systematic effects with typical relative uncertainties (parts in 10^{15}) for caesium fountain and thermal beam standard. (Compiled from data presented in Ref. [3].)

Effect	beam standard	fountain
Quadratic Zeeman	1	0.1
Quadratic Doppler	1–3	0.1
Cavity phase difference	4–10	0.2–0.5
Detuning of the μ-wave cavity	0.3–1	0.1
Asymmetry of Zeeman populations	0.2–2	0.1–0.5
AC Stark (thermal radiation)	1	0.3
AC Stark (fluorescence)	0–1	0.1
Spin-exchanging collisions	—	0.5–1.4

In Table I, the major systematic effects and their uncertainties for caesium fountains and thermal beam standards are compared. The inherent advantage of the use of atoms with small thermal velocities (1–2 cm/s) in the fountain is the reduction of the uncertainty contribution from most frequency shifting effects, the second order Doppler shift (time dilation) being the most obvious. The Ramsey method, although developed for the thermal beam device, introduces smaller uncertainties in the fountain, where the atoms pass twice through a single microwave cavity and hence the problem of the phase difference between the two arms of the Ramsey cavity is absent. There remains a distributed phase shift (first order Doppler shift) across the aperture of the single cavity, but it is smaller for slow atoms. The uncertainty contributions from cavity detuning and the population asymmetry of the Zeeman sublevels are negligible, as a result of the narrower atomic resonances. Further, the narrower resonances allow a much smaller magnetic field to be used, than is the case for beam standards, in order to resolve the Zeeman structure. Thus the quadratic Zeeman shift and its uncertainty is reduced.

The AC Stark effect due to thermal radiation, is not smaller in the fountain, but recent experiments done both in a fountain and in a thermal beam device have provided new data, allowing a better estimate of the uncertainty of the effect [30, 31].

The dominant source of systematic uncertainty in caesium fountains is a frequency shift caused by spin-exchanging collisions, usually neglected in the uncertainty budget for thermal beam standards.

4. Cold collisions

The last two decades have witnessed several elegant experiments in which investigations of single channels of collisional reaction were performed and the possibilities of the manipulation of the process with laser light were explored [32]. The dominant channel giving rise to a collisional frequency shift in the atomic fountain is the process in which two atoms approaching each other exchange their electrons or spins.

Cold collisions (*i.e.* between atoms with a temperature in the micro-Kelvin range) have several unique properties. The temperature, and thus the momentum, of the atoms is small so the de Broglie wavelength can be as high as hundreds of nanometres. Thus the "size" of the cold atom is comparable with, or even larger than, the range of interatomic potential. The collisions are dominated by low angular momentum processes. Because of the small kinetic energy of the colliding atoms only the first few partial waves (s, p and d) contribute significantly to the cross section, which can be seen in photoassociation spectra [33]. As the atoms become cooler the

collision energy approaches zero but the collision rate for the dominating s-wave inelastic process remains finite and reaches a constant, independent of the temperature of the atoms. This behaviour is known as the Wigner threshold law or $1/v$ rule [34].

The key quantity, which describes the effect of collision on the fountain performance, is the phase shift. This shift is proportional to the atomic density and the rate of the collisions. The first calculations of the cross section for the spin exchange process were performed in the context of the hydrogen maser [35]. In particular, the group from Eindhoven has shown that the influence of hyperfine structure on the collisional shift becomes significant for temperatures below 1 K. The first estimates [36] for the caesium fountain gave a relative shift of the order $10^{-22}\ n/\mathrm{cm}^{-3}$, where n is the atomic density in units of cm^{-3}. The calculated rate of the process (momentum equal to zero and s-wave scattering) increased as the temperature of the atoms was reduced but, in the range of 10^{-6} K, it reached the limit.

In an experiment performed by Gibble and Chu the relative shift of $-1.4 \times 10^{-21}\ n/\mathrm{cm}^{-3}$ was measured for a density of $10^9\ \mathrm{cm}^{-3}$ at 3 μK [37]. This was confirmed by a more accurate measurement at smaller densities, performed by the group at LPTF [38]. According to calculation, the value obtained in these experiments is nearly equal to the predicted threshold for $T \to 0$ [36].

The accuracy of the calculations of the collisional cross-section and subsequently the collisional shift is limited by the knowledge of the details of the interaction potential between two colliding atoms. Recently a series of high-resolution Feshbach resonance spectra for caesium were obtained [39]. These results were used to recalculate the frequency shift and its dependence on collisional energy (*i.e.* temperature) [40]. The calculations showed completely different behaviour of the shift as the temperature is reduced. Figure 4 shows both calculated and measured values of the clock shift. The shift has a broad minimum around 400 nK and it crosses zero around 100 nK. It approaches the flat Wigner regime for temperatures less than 0.1 nK (not shown in the figure). The measurements so far have not reached the region where the significant variations of the shift are predicted to occur.

Thus a further experimental effort to cool the atoms below 1 μK is highly desirable in order to verify the theoretical predictions. An issue to be considered, is the optimum range of the temperatures at which the fountain should operate, either close to flat parts of the curve from figure 4, or around the 100 nK region, where the shift is small, but more sensitive to temperature variations.

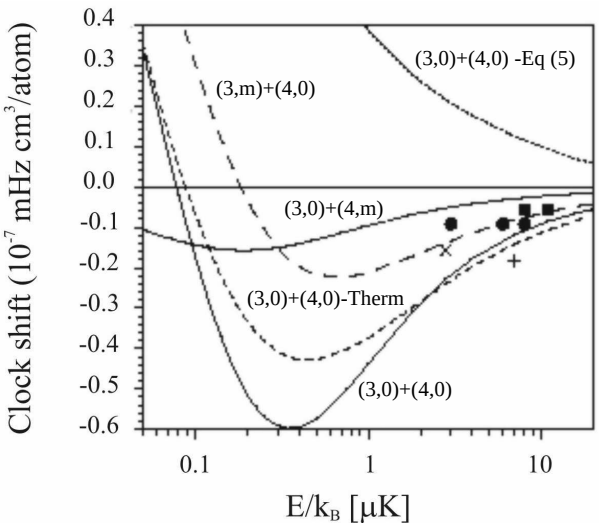

Fig. 4. Calculated frequency shift due to collisions between caesium atoms in $F = 3$ and $F = 4$. Curves "$(3,0) + (4,m)$" and "$(3,m) + (4,0)$" assume that all Zeeman sublevels are initially evenly populated. Curve "$(3,0) + (4,0)$-Therm" includes average over Maxwell–Boltzman distribution of atomic velocities in the launched cloud. From Ref. [40].

5. Further cooling

It follows from the previous section that cooling the atoms to lower temperatures does not straightforwardly reduce the collisional frequency shift. It is however desirable to reduce the temperature of the atomic cloud during the launch: the smallest aperture of the system constraining the atomic trajectories is a hole in the microwave cavity which has a diameter of 10 mm or less, to restrict the distributed phase shift. For a thermally expanding cloud of atoms at launch temperatures of 2–5 μK, only 5–10% of the atoms can fall through this aperture to return to the detection region. This means that 10–20 times more atoms contribute to the collisional shift than to the fountain signal. This trade-off between stability and accuracy could be improved for lower velocity spreads, as either fewer atoms (smaller frequency shift) could be launched to maintain the S/N ratio, or for a given initial number of atoms a higher S/N could be obtained. Several experiments aiming to achieve temperatures lower than those in a standard molasses have been performed.

5.1. Grey molasses

The cooling mechanism in a conventional "bright" optical molasses relies on the Sisyphus effect and uses lasers red detuned from a $F \to F+1$ cycling transition. The minimum temperature depends on the fluorescence rate and photon multiple scattering. Tuning the laser to $F \to F$ or $F \to F-1$ transition results in some atomic states of the ground state manifold being not coupled to the laser light [41]. By optical pumping, atoms with low momentum (of the order of single photon recoil) accumulate into those states where their fluorescence is reduced [42]. These states are not dark states, as they are motionally coupled to the bright states, hence the name "grey molasses".

Experimentally, as the cooling requires blue detuning of the laser beams, direct capture of the atoms from a vapour is not possible and the grey molasses is applied after an initial phase of bright molasses. A temperature of 1.1 μK was measured after 1 ms cooling for atomic densities below 10^9 cm^{-3} [43]. The temperature was also found to increase linearly with the density at a rate of 0.6 μK/(10^{10} atoms/cm^{-3}).

5.2. Raman cooling

Raman cooling also relies on accumulation of atoms with low momenta (even lower than photon-recoil) while those atoms with higher momenta undergo cycles of optical pumping and Raman transfer. During an optical pumping pulse atoms scatter photons in a random direction having a chance to end up in an arbitrarily narrow class near zero momentum. Velocity selective Raman pulses are used to "recycle" those atoms with momenta falling outside the narrow class. Raman pulses of specially tailored form were used to avoid excitation of the slowest atoms [44, 45]. An experiment with Cs atoms in one dimension reached temperatures as low as 3 nK [45]. Cooling in two and three dimensions is also possible [46], but requires a rather complicated and long sequence of optical pulses. In the fountain the cooling has to be applied after the launch and completed within 2–3 ms because of laser beam size limitations.

A simpler experiment where only two Raman pulses are used to *select* atoms with the smallest velocities in the horizontal plane is more applicable to the fountain [47, 48]. An atomic sample with 'horizontal' temperature of 100 nK can be created in a fraction of a millisecond; the velocity spread along the vertical is not relevant, as it does not reduce the number of detected atoms. As this is not a cooling process and the majority of faster atoms are removed, this loss would have to be compensated for by loading more atoms into the MOT (*e.g.* from a beam).

5.3. Adiabatic cooling

Adiabatic cooling can be performed if the atoms are initially held in a periodic potential well, or optical lattice. The populations of the different vibrational levels of the well are proportional to the Boltzmann factor $\exp\{-\hbar\omega'/kT\}$, where $\hbar$ and k are the Planck and Boltzmann constants respectively, ω the vibrational frequency, and T the vibrational temperature. With a gradual (adiabatic) reduction of the lattice potential, achieved by reducing the intensity of lasers creating the lattice, the energies of the vibrational levels are lowered [49]. The adiabaticity condition is fulfilled if the rate of change of the energy of the levels is slow compared to the frequency of oscillation of an atom within a vibrational level. More precisely, the Boltzmann factor remains constant with decreasing ω only if T decreases as well. This uncomplicated experimental scheme is now routinely used in caesium fountains, where the cooling beams provide a quasi-instantaneous optical lattice. A linear reduction in intensity is applied for 1 ms leaving the atoms at temperatures around 1 μK [50, 51].

5.4. Raman sideband cooling

The group in Stanford has recently developed a possible route for cooling atoms to very low (sub-μK) temperatures [52], which is attractive in the context of testing the predicted dependence of the collisional frequency shift on temperature in the sub μK range. The cooling comprises two stages. Atoms in an optical lattice are transferred to the lowest vibrational level by Raman sideband cooling and then released from the lattice adiabatically, as described above.

Atoms distributed among different vibrational levels of the potential wells of the lattice are optically pumped to one Zeeman sublevel of the ground state ($F = 3,\ m_F = 3$ for caesium) (I in figure 5). A small magnetic field (5–6 μT) brings three different vibrational states of three magnetic sub-levels into degeneracy $|F = 3,\ m_F = 3, n\rangle$, $|F = 3, m_F = 2,\ n-1\rangle$, and $|F = 3,\ m_F = 1, n-2\rangle$. Strong Raman coupling equalizes populations of these states, effectively transferring the atoms from vibrational state n ($m_F = 3$) to states $n-1$ ($m_F = 2$) and $n-2$ ($m_F = 1$). Additional laser beams optically pump the atoms back to the $m_F = 3$ sublevel (II). This optical pumping does not change the vibrational quantum number so, after one cycle, atoms are moved to the $|F = 3,\ m_F = 3, n-2\rangle$ state (III). Subsequent cooling cycles (II–III) transfer the atoms to the lower vibrational levels until the ground state is finally reached [53]. The Stanford group implemented a degenerate scheme, where the laser beams creating the lattice potential also provided the Raman coupling. To make matters simpler experimentally, the MOT lasers can be used. In a caesium fountain this technique can either be

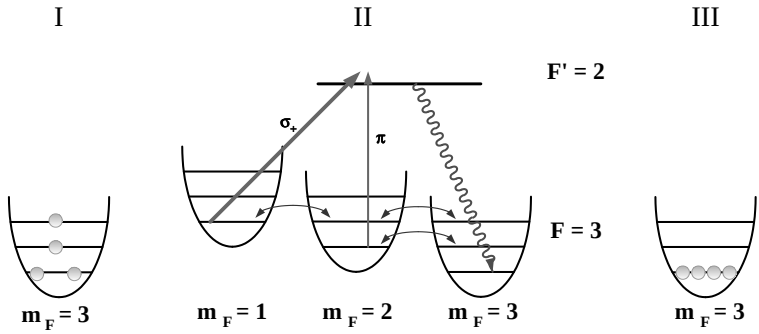

Fig. 5. Degenerate Raman sideband cooling. Atoms are transferred to the lowest vibrational state by optical pumping and Raman coupling between vibrational states for different Zeeman sublevels.

applied after the launch, where atoms are cooled in a co-moving lattice, or it could be used to launch the atoms. The first approach seems to be more effective: atoms moving at 5 m/s were cooled down to 150 nK [52].

6. Future prospects for microwave standards

Caesium fountains now have an accuracy of about 1×10^{-15} and can reach a stability better than 1×10^{-15} in 10^4 seconds or less [54]. A small number of effects of similar size contribute most of the systematic uncertainty: distributed cavity phase, other Zeeman sublevels, blackbody radiation, and cold collisions. The last of these is the largest. In addition, a reduction in the cold collisional shift can result in improved stability. There is potential to improve fountain performance further both in systematic uncertainty and stability.

6.1. Systematic shifts

Various techniques for lowering the temperature of the atoms have been reviewed in Section 5. Schemes have also been developed to reduce the average density without using exotic cooling schemes, whilst maintaining the average number of detected atoms. Various forms of "juggling", where several clouds of atoms are simultaneously in ballistic flight have been proposed. Juggling schemes can be constructed where there is little interaction between the atom clouds, which may be of individually lower density. The clouds may be launched to different heights so as to avoid passage of one cloud through another [55, 56] or multiple clouds to the same height [57]. The latter has been demonstrated experimentally to perform studies of quantum scattering of ultra-cold atoms. A related approach is that of a continuous

cold beam, launched from a modified MOT [58]. Atoms are launched continuously on a parabolic path with a small horizontal velocity component, by moving molasses and are cooled to about 5 μK. Stability comparable to pulsed fountain devices has been demonstrated. All these departures from the conventional fountain have in common that, to control AC Stark shifts, carefully designed light baffles are necessary, to screen atoms undergoing the Ramsey interaction from fluorescence due to the cooling lasers.

Recent measurements of the cold collisional shift in rubidium show that it is 30 to 50 times smaller than in caesium [59, 60]. The reproducibility and long-term stability of a rubidium fountain can thus be expected to be better than in caesium. Furthermore, it has been shown that the collisional shift in rubidium can be compensated for by means of the so-called cavity pulling effect. The total field in the cavity is phase shifted by the microwave radiation from the atoms themselves, giving rise to a density dependant frequency shift. The cavity resonance parameters can be chosen such that these two shifts cancel one another, so as to offer further improvement to long-term stability [59].

Operating a fountain at lower temperatures can, in principle, reduce the blackbody radiation effect. For example, at 273 K the shift in a blackbody is 30% smaller when compared to 298 K. Cryogenic operation of a fountain may reduce the uncertainty in the blackbody shift to parts in 10^{-17} provided a blackbody field can be approximated.

There are a number of approaches to reducing the distributed cavity phase shift (first order Doppler effect). These include a reduction in the velocity of the atoms as they pass through the microwave field, reduction of the size of the travelling wave component, improved homogeneity of the phase distribution across the aperture of the microwave cavity, and better retracing of the atom path. The latter would be improved by the use of much colder atoms. The use of higher Q cavities might be explored in order to reduce the travelling wave component, but the Q is limited by the atom density, and higher Q makes the effect of cavity pulling harder to control.

6.2. Stability

Given that the atom number has been set so as to reach the desired cold collision uncertainty, the stability may be increased by a reduction in noise or an increase in the Q. It has been suggested that the quantum projection noise could be reduced by the use of quantum correlated atoms [28]. Local oscillators with stability at the 10^{-14} level at 1 second are required, if a future fountain is to reach its uncertainty limit at the 10^{-16} level in no more than 1 day of averaging. In addition to cryogenic sapphire a technique with great promise is frequency synthesis by mixing the optical comb frequencies of a mode-locked femtosecond laser described in Section 7 [61].

A Ramsey fringe width substantially below a second is impractical in the presence of gravity. However there are experiments in preparation to exploit the microgravity environment of space. Interaction times of some 10 seconds are expected and some experiments are well advanced, with scheduled operation in 2005 [62]. The interaction time in microgravity is limited by the expansion of the atom cloud leading to loss of S/N overtaking the improvement to the Q. It is planned to overcome this by launching multiple atomic clouds in a manner similar to that described above.

6.3. Frequency transfer

Comparison of the frequency of fountains in standards laboratories can be accomplished using satellite time transfer. Two-way satellite time and frequency transfer has been demonstrated with uncertainties at about 10^{-15}[63]. Increased bandwidth and more data collection through continuous operation has the potential to improve on this. A transportable caesium fountain has been constructed and can be used at the 10^{-15} level [64].

7. Optical frequency standards

In order to go beyond the level of frequency stability projected for the best caesium or rubidium fountain microwave standards, optical frequency standards based on forbidden transitions in laser-cooled atoms and ions are being developed at a number of laboratories world-wide. The frequency of an optical transition is of the order of 10^5 times greater than that of the ground state hyperfine splitting in caesium or rubidium. Some of the atom or ion species used for optical frequency standards have forbidden transitions with a natural linewidth of 1 Hz or less, comparable to the width of the Ramsey fringe in a microwave fountain. This increase in the Q of the transition should in principle yield a similar increase in relative frequency stability.

The majority of laser-cooled optical frequency standards have been developed with the initial object of providing improved standards for realisation of the SI metre. The SI metre is directly related to the SI second through the assigned value for the speed of light in vacuum. However, because precision length metrology is performed by optical interferometry and because of the historical difficulty of directly comparing microwave and optical frequencies, there has been a need for secondary frequency standards at optical frequencies. This has been met through the development of lasers stabilised to saturated absorption features in gases or vapours, such as molecular iodine. In the visible region of the spectrum, the relative frequency reproducibility of these molecular standards is limited to a few parts in 10^{11}. The *mis en pratique* of the realisation of the metre [65] lists the optical frequency standards which have been adopted by the CIPM, including laser-cooled

standards based on ^{40}Ca and $^{88}Sr^{+}$. Neither of these species is necessarily the most promising candidate for the ultimate optical frequency standard but either is probably the most fully characterised of its type. The brief survey which follows is confined to those atom and ion species currently being pursued as laser-cooled standards, neglecting some interesting systems which are at present only being studied in thermal beam experiments, of which the most notable is atomic hydrogen [66].

7.1. Cold atom optical frequency standards

An optical fountain frequency standard using laser-cooled neutral atoms was proposed even before the demonstration of the caesium microwave fountain [67, 68]. Most of the standards which are being developed make use of Ramsey interferometry on a narrow-linewidth optical transition such as the $^1S_0$–$^3P_1$ intercombination line in the alkaline earth elements, magnesium, calcium, and strontium (Fig. 6(a)). Calcium is the most fully developed of these systems as a frequency standard, with MOT-based devices at PTB [69] and NIST [70]. These devices build on earlier work using Ramsey interferometry on a calcium thermal beam. Laser cooling of these

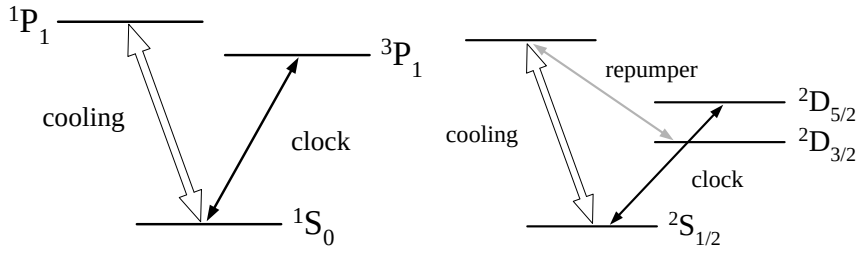

Fig. 6. Representative term diagrams for laser-cooled optical frequency standards using (a) alkali earth atoms *e.g.* ^{40}Ca or (b) alkali metal-like ions *e.g.* $^{88}Sr^{+}$.

elements can be achieved on the $^1S_0$–$^1P_1$ resonance transition; although this transition is rather weaker and at shorter wavelength than the equivalent $^2S_{1/2}$–$^2P_{3/2}$ transition of the alkali metals rubidium and caesium, laser cooling and trapping in the MOT configuration has been achieved for all three of these elements. The most abundant isotope of calcium, ^{40}Ca, being an even isotope with zero nuclear spin, lacks hyperfine structure. This prevents the sub-Doppler cooling mechanisms used to obtain very low temperatures with the alkali metals from working. The Doppler-limited width of transitions in atoms in the MOT remains much greater than the 400 Hz natural linewidth of the 657 nm intercombination line. Ramsey fringes in the fluorescence intensity of spontaneous emission from the $^3P_1$ state are obtained through Doppler-free excitation in a Ramsey–Bordé atom interferometer [71]. A laser

at 657 nm is pre-stabilised by locking to a stable high-finesse Fabry–Perot cavity in order to achieve a linewidth of the order of the natural linewidth [72]. Ramsey fringe widths of 200 Hz have been obtained, but the signal-to-noise is poor. At a fringe width of around 1 kHz, a short term fractional frequency stability of $4 \times 10^{-15}\tau^{-1/2}$ has been reported [73] with a projected improvement of a factor of 40 [70].

The intercombination line in strontium is rather broader than in calcium, with 7 kHz natural linewidth. The larger transition rate makes second-stage cooling to the recoil limit on this transition more feasible [67]. Strontium can be trapped in a MOT using the $^1S_0$–$^1P_1$ resonance transition at 461 nm and can be further sideband cooled on the 689 nm intercombination transition [74–76]. This is the first step towards obtaining low enough atom temperature to be able to exploit the longer interaction time attainable using the fountain geometry. Although the strontium intercombination line is relatively broad, this species has two other narrow transitions which may be candidates as optical frequency standards, the $^1S_0$–$^1D_2$ two-photon transition at 993 nm, with 500 Hz linewidth, and the very weak $^1S_0$–$^1P_2$ magnetic quadrupole ($M2$) transition at 671 nm, which has a linewidth of about 1 mHz. Strontium also has an odd isotope, ^{87}Sr, which could be cooled to the recoil limit on the resonance transition. A two-photon transition with 0.6 Hz linewidth at 661 nm in ^{109}Ag has also been identified as a possible standard and work towards a silver fountain is in progress [77–78].

Potential limitations to the accuracy obtainable with optical frequency standards using the Ramsey–Bordé technique include the stringent limit placed on shifts of the optical phase between the Ramsey interactions in the interferometer and also the cold collisional shift [69]. The AC Stark shift is also problematic, especially for two-photon transitions.

7.2. Trapped ion optical frequency standards

A single ion, stored in an electrodynamic trap, can be laser cooled to the Lamb–Dicke regime, in which the first-order Doppler shift due to the ion's motion is eliminated. The detection of a weak transition is facilitated by the use of the quantum jump technique. (For a review of ion trapping techniques, see [79].) It has been speculated that a trapped ion optical frequency standard could yield a reproducibility of 1 part in 10^{18} [80]. Electric quadrupole (E2) transitions, with linewidths of about 1 Hz, are usually used as the spectral reference. A number of different ion species are being investigated to assess their suitability as standards. Ions with alkali-like electronic structure (figure 6(b)), which include Ca^+, Sr^+, Ba^+, Yb^+, and Hg^+, have a strong $^2S_{1/2}$–$^2P_{1/2}$ transition which permits high resonant scattering rates, making them well suited for laser cooling, although in general the electric

dipole (E1) branching decay of the $^2P_{1/2}$ level to the lower-lying $^2D_{3/2}$ level results in the need for an additional repumping laser to maintain the cooling cycle. The reference transition most commonly addressed is the quadrupole $^2S_{1/2}$–$^2D_{5/2}$ transition. An odd isotope, with $m_F = 0 - m_F = 0$ Zeeman components, is preferable; in particular, $^{199}Hg^+$ and $^{171}Yb^+$ have nuclear spin $^1/_2$ and therefore comparatively simple hyperfine structure.

The strontium ion is particularly attractive as a practical optical frequency standard [81, 82] as all the wavelengths required can be obtained using compact diode laser systems. The cooling and repumping transitions are at 422 and 1092 nm whilst the $5s^2S_{1/2}$–$4d^2D_{5/2}$ reference transition is at 674 nm. At NPL, three similar traps have been compared, providing the first tests of the reproducibility and stability of ion-trap optical frequency standards [83]. As a frequency standard, $^{88}Sr^+$ suffers from the disadvantage of being an even isotope and hence subject to first order Zeeman shifts. The trapping of $^{87}Sr^+$, which has nuclear spin $^9/_2$ and hence a rather complex hyperfine structure, is also being studied at NPL [84].

The ytterbium ion is the most versatile of the various ion species under consideration, having reference transitions in the visible, infrared, and microwave regions of the spectrum. Recent work has used the odd isotope $^{171}Yb^+$. This ion has three candidate transitions in the optical spectrum. The 411 nm $^2S_{1/2}$–$^2D_{5/2}$ transition was originally proposed by Werth [85] and has been investigated as an optical frequency standard at NPL [86]. A standard based on the 435 nm $^2S_{1/2}$–$^2D_{3/2}$ transition has been constructed at PTB [87]. At NPL recent work has concentrated on the 467 nm $^2S_{1/2}$–$^2F_{7/2}$ electric octupole (E3) transition which is the narrowest known resonance in the optical spectrum, with $Q \sim 10^{24}$, the $^2F_{7/2}$ level having a radiative lifetime of ten years [88, 89].

Mercury ions have been extensively studied by the NIST group [70]. If the full potential of optical standards is to be realized, lasers with linewidth less than the natural linewidth of the reference transition are required. The NIST group has stabilized the output of a dye laser at 563 nm to obtain 0.6 Hz linewidth [90]. This radiation is frequency doubled to 282 nm, the wavelength of the $^2S_{1/2}$–$^2D_{5/2}$ transition in $^{199}Hg^+$. An interaction time limited linewidth of 6.7 Hz has been observed on this transition [91].

In addition to alkali-like ions, forbidden transitions in ions of group III A elements also have potential as optical frequency standards [92], with single, laser cooled indium ions being trapped by groups at the University of Washington [93] and at Garching [94]. In^+ has a similar electronic structure to the alkaline earth atoms such as calcium. The proposed reference transition is not the intercombination line but the strongly forbidden $^1S_0$–$^3P_0$ transition, which, in isotopes with non-zero nuclear spin, has a small E1 decay

rate due to hyperfine mixing with states having electron angular momentum $J = 1$. Because both levels have $J = 0$, and hence no electronic quadrupole moment, the transition is free of the quadrupole shift arising from coupling to the trapping electric field gradient, which is one of the limiting systematic effects for alkali-like ions. Because the $^1S_0$–$^1P_1$ transition is in the VUV at 159 nm, cooling has to be performed on the 231 nm intercombination line, whilst the 1.1 Hz natural linewidth reference transition is at 236 nm.

7.3. Femtosecond optical frequency comb

Until the beginning of the present century, the precision intercomparison of optical and microwave frequency standards could only be achieved by means of a harmonic frequency chain. This consists of a number of oscillators at progressively higher frequencies (microwave Gunn oscillators and klystrons, far-infra-red alcohol lasers, CO_2 lasers, *etc.*) phase-locked through electronic beat frequencies obtained in fragile harmonic-mixing devices (metal-insulator-metal diodes, Schottky diodes). The complexity of these chains has limited their construction to a handful of laboratories around the world. The multiplication of the microwave frequency to very high harmonic introduces sources of noise which limit the precision which can be achieved. The most precise measurement of a laser-cooled optical frequency standard which has been made using a harmonic frequency chain is that of the ^{40}Ca standard at PTB, with a relative uncertainty of 1×10^{-12} [95].

This situation has been revolutionised by the advent of optical frequency combs based on mode-locked femtosecond lasers. The concept that, in the frequency domain, the train of pulses from a mode-locked laser corresponds to a grid or "comb" of discrete laser frequencies, uniformly spaced by the repetition rate of the laser pulses, is a quarter of a century old [96]. However, it is only within the last few years that three developments have come together to produce a metrological tool of unprecedented utility. The first is mode-locking of solid state lasers such as Ti:sapphire by the Kerr effect in the laser crystal [97]. Allied to this is the development of all-solid-state frequency-doubled Nd:YAG and Nd:YVO pump lasers with low amplitude noise. In the first optical frequency measurement using a femtosecond laser comb, the bandwidth of the comb generated by a mode-locked Ti:sapphire laser producing 75 fs pulses was about 20 THz [98]; the final development is the use of self-phase-modulation of the pulses in photonic crystal fibre [99] or microstructure fibre [100] to broaden the comb to cover over 300 THz or more than one octave in optical frequency [101, 102]. The comb frequencies are uniformly spaced by the pulse repetition rate frequency f_R which corresponds to the round-trip time of the pulse within the laser cavity. This

frequency can be compared or stabilised to a microwave frequency standard to high precision. However, the absolute frequencies of the comb modes are not integer multiples of f_{R}. For each round trip within the laser cavity, the difference between the phase and group velocities results in a phase difference $\Delta\phi$ accumulating between the phase of the optical carrier and the pulse envelope (figure 7). In the comb due to the train of pulses emitted from the cavity at f_{R}, this phase difference gives rise to a frequency offset $f_0 = \Delta\phi\ f_{\mathrm{R}}/2\pi$, commonly called the carrier envelope offset frequency. Using an octave-span comb, f_0 can be directly measured as the rf beat frequency between modes from the green region of the comb and the second harmonic of modes from the infra-red region of the comb [101]. The frequency ν of laser stabilised to an optical reference is thus determined from its rf beat frequency Δ with an adjacent mode of the comb, the frequencies f_{R} and f_0, and the mode number m:

$$\nu = m f_{\mathrm{R}} \pm f_0 \pm \Delta\,,$$

where m and the signs of the beat frequencies are determined experimentally, requiring that the optical frequency ν is known *a priori* to an accuracy of a few tens of MHz.

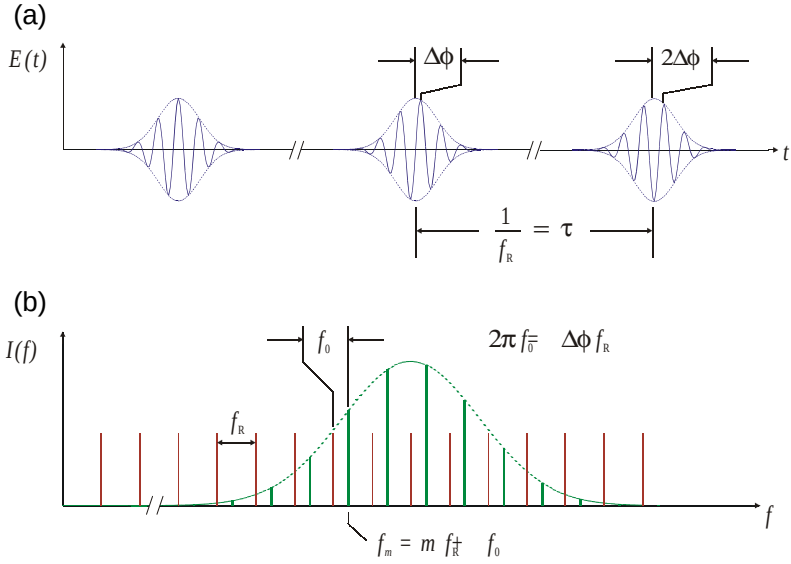

Fig. 7. The pulse train from a mode-locked femtosecond laser represented in (a) the time domain and (b) the frequency domain, illustrating the generation of a frequency comb with modes at frequencies f_m determined by the pulse repetition rate f_{R} and the carrier envelope offset frequency f_0.

Femtosecond combs are now being used to compare the frequencies of many of the optical frequency standards described above with microwave standards. At NIST and PTB, the Hg^+ [103] and Yb^+ [104] ion traps and Ca MOT standards [103, 105] have been compared to caesium fountains. The ion trap comparisons have been made with a fractional frequency uncertainty of 1×10^{-14}. At NPL, femtosecond comb measurements of the Sr^+ and Yb^+ ion traps are underway [106]. Alongside these measurements, the uncertainty and instability introduced into the optical-to-microwave comparisons by the comb is being investigated. Comparison of two comb-based frequency chains has shown a fractional accuracy of 5×10^{-16} [102] and a fractional instability of $\leq 6.3 \times 10^{-16}$ [107]. These measurements provide confidence that the femtosecond comb will not be a limitation to the operation of a cold atom or ion frequency standard as an optical clock, *i.e.*as a frequency standard producing an microwave output which can input to the generation of a timescale. Such operation has been demonstrated at NIST using Hg^+ [108], by stabilising the comb to the optical, rather than the microwave standard.

8. Conclusions

The application of cold atom techniques to caesium primary frequency standards has enabled the fountain geometry to be implemented, nearly four decades after it was first proposed. The use of atoms with thermal velocities of 1 cm/s or less, together with the atom path reversal that is intrinsic to the fountain geometry, leads to large reductions in several systematic frequency shifts. These advances have, in the course of about a decade, produced an order of magnitude improvement in the realisation of the SI second, compared to thermal beam caesium standards. The limiting frequency shift in the caesium fountain is that due to spin exchange collisions between cold atoms.

The application of novel cooling techniques may lead, in the next decade, to a further improvement in accuracy and stability in microwave atom fountains, towards 1×10^{-16}. However, the femtosecond comb now provides an accurate means for linking optical and microwave frequencies. Advances in the accuracy and stability of measurements on optical frequency standards using forbidden transitions in laser-cooled neutral atoms and trapped ions can now be readily verified by comparison both with each other and with the caesium fountain. Hence, it is likely that there will be a number of highly stable optical standards created, having better reproducibility than microwave fountains. Frequency ratios between some of these will be known to greater accuracy than the realisation of the SI second.

The richness of possibilities ensures that the application of ultracold atoms for ultrastable frequency standards in both the microwave and optical regions of the spectrum will continue to be an exciting field in the coming years.

The authors thank G.P. Barwood for careful reading of the manuscript, P.S. Julienne for permission to use figure 4 and H.S. Margolis for supplying figure 7.

REFERENCES

[1] P. Fisk, *Rep. Prog. Phys.* **60**, 761 (1997).

[2] A. Luiten (ed), *Frequency Measurement and Control — Advanced Techniques and Future Trends*, Springer, Berlin 2001.

[3] A. Bauch, H. Telle, *Rep. Prog. Phys.* **65**, 789 (2002).

[4] I.I. Rabi, S. Millman, P. Kusch, J.R. Zacharias, *Phys. Rev.* **55**, 526 (1939).

[5] N.F. Ramsey, *J. Res. NBS* **88**, 301 (1983).

[6] N.F. Ramsey, *Phys. Rev.* **78**, 695 (1950).

[7] J. Sherwood, H. Lyons, R. McCracken, P. Kusch, *Bull. Am. Phys. Soc.* **27**, 43 (1952).

[8] L. Essen, J.V.L. Parry, *Nature* **176**, 280 (1955).

[9] W. Markowitz , R.G. Hall, L. Essen, J.V.L. Parry, *Phys. Rev. Lett.* **1**, 105 (1958).

[10] A. Bauch, B. Fischer, T. Heindorff, P. Hetzel, P. Petit, R. Schroder, P. Wolf, *Metrologia* **37**, 683 (2000).

[11] D.W. Allan, *Proc. IEEE* **54**, 221 (1966).

[12] J. Vanier, C. Audoin, *The Quantum Physics of Atomic Frequency Standards*, 1st ed., Adam Hilger, Bristol 1989, p. 798.

[13] G.D. Rovera, E. de Clercq, A. Clairon, *IEEE Transactions on Ultrasonics Ferroelectrics and Frequency Control*, **UFFC-41**, 245 (1994).

[14] J.H. Shirley, W.D. Lee, R.E. Drullinger, *Metrologia* **38**, 427 (2001).

[15] S. Chu, *Rev. Mod. Phys.* **70**, 685 (1998); C. Cohen-Tannoudji, *Rev. Mod. Phys.* **70**, 707 (1998); W.D. Phillips, *Rev. Mod. Phys.* **70**, 721 (1998).

[16] M.A. Kasevich, E. Riis, S. Chu, R.G. de Voe, *Phys Rev. Lett.* **63**, 512 (1989).

[17] A. Clairon, C. Salomon, S. Guellati, W.D. Phillips, *Europhys. Lett.* **16**, 165 (1991).

[18] E. Riis, D.S. Weiss, K.A. Moler, S. Chu, *Phys. Rev. Lett.* **64**, 1658 (1990).

[19] A. Clairon, P. Laurent, G. Santarelli, S. Ghezali, S. Lea, M. Bahoura, *IEEE Trans. Instrum. Meas.* **44**, 128 (1995).

[20] S. Weyers, U. Huebner, B. Fischer, R. Schroeder, C. Tamm, A. Bauch, *Metrologia* **38**, 343 (2001).

[21] D. Meekhoff, S. Jefferts, M. Stepanovic, T. Parker, *IEEE Trans. Instrum. Meas.* **50**, 507 (2001).

[22] E. Burt, C. Ekstrom, T Swanson, 2001 Proc. 15$^{\text{th}}$ Eur. Frequency and Time Forum, p. 67.

[23] D. Henderson, S. Lea, K. Szymaniec, P. Whibberley, 2001 Proc. 15$^{\text{th}}$ Eur. Frequency and Time Forum, p. 398.

[24] F. Levi, A. Godone, L. Lorini, D. Calonico, G. Brida, 2001 Proc. 15$^{\text{th}}$ Eur. Frequency and Time Forum, p. 104.

[25] G. Constanzo, C. Calosso, A. De Marchi, 2001 Proc. 15$^{\text{th}}$ Eur. Frequency and Time Forum, p. 416.

[26] Li Tianchu, Li Mingshou, Huang Bingying, Qian Jin, Lin Pingwei, *Proc. 2000 IEEE Int. Frequency Control Symposium.*

[27] A. Clairon, G. Santarelli, S. Ghezali, P. Laurent, S. Lea, M. Bahoura, E. Simon, S. Weyers, K. Szymaniec, *Proc. 5th Symp. on Frequency Standards and Metrology*, World Scientific, Singapore 1996, pp 49-59.

[28] G. Santarelli, C. Audoin, A. Makdissi, P. Laurent, G.J. Dick, A. Clairon, *IEEE Trans. Ultrason. Ferroelectr. Freq. Control.* **45**, 887 (1998).

[29] G. Santarelli, P. Laurent, P. Lemonde, A. Clairon, A.G. Mann, S. Chang, A.N. Luiten, C. Salomon, *Phys. Rev. Lett.* **82**, 4619 (1999).

[30] A. Bauch, R. Schroder, *Phys. Rev. Lett.* **78**, 622 (1997).

[31] E. Simon, P. Laurent, A. Clairon, *Phys. Rev.* **A57**, 436 (1998).

[32] J. Weiner, V.S. Bagnato, S. Zilio, P.S. Julienne, *Rev. Mod. Phys.* **71**, 1 (1999).

[33] H.M.J.M. Boesten, C.C. Tsai, J.R. Gardner, D.J. Heinzen, B.J. Verhaar, *Phys. Rev.* **A55**, 636 (1997).

[34] E.P. Wigner, *Phys. Rev.* **73**, 1002, (1948) and references therein.

[35] B.J. Verhaar, J.M.V.A. Koelman, H.T.C. Stoof, O.J. Luiten, *Phys. Rev.* **A35**, 3825 (1987); H.T.C. Stoof, J.M.V.A. Koelman, B.J. Verhaar, *Phys. Rev.* **B38**, 4688 (1988) and references therein.

[36] E. Tiesinga, B.J. Verhaar, H.T.C. Stoof, D.van Bragt, *Phys. Rev.* **A45**, R2671 (1992).

[37] K. Gibble, S. Chu, *Phys. Rev. Lett.* **70**, 1771 (1993).

[38] S. Ghezali, Ph. Laurent, S.N. Lea, A. Clairon, *Europhys. Lett.* **36**, 25 (1996).

[39] Ch. Chin, V. Vuletic, A.J. Kerman, S. Chu, *Phys. Rev. Lett.* **85**, 2717 (2000).

[40] P.J. Leo, P.S. Julienne, F.H. Mies, C.J. Williams, *Phys. Rev. Lett.* **86**, 3743 (2001).

[41] A. Aspect, E. Arimondo, R. Kaiser, N. Vansteenkiste, C. Cohen-Tannoudji, *Phys. Rev. Lett.* **61**, 826 (1988).

[42] G. Grynberg, J.-Y. Courtois, *Europhys. Lett.* **27**, 41 (1994).

[43] D. Boiron, A. Michaud, P. Lemonde, Y. Castin, C. Salomon, S. Weyers, K. Szymaniec, L. Cognet, A. Clairon, *Phys. Rev.* **A53**, R3734 (1996).

[44] M. Kasevich, S. Chu, *Phys. Rev. Lett.* **69**, 1741 (1992).

[45] J. Reichel, F. Bardou, M.B. Dahan, E. Peik, S. Rand, C. Salomon, C. Cohen-Tannoudji, *Phys. Rev. Lett.* **75**, 4575, (1995).

[46] N. Davidson, H.J. Lee, M. Kasevich, S. Chu, *Phys. Rev. Lett.* **72**, 3158 (1994).

[47] M. Kasevich, D.S. Weiss, E. Riis, K. Moler, S. Kasapi, S. Chu, *Phys. Rev. Lett.* **66**, 2297 (1991).

[48] K. Szymaniec, S. Ghezali, L. Cognet, A. Clairon, *Opt. Commun.* **144**, 50 (1997).

[49] A. Kastberg, W.D. Phillips, S.L. Rolston, R.J.C. Spreeuw, P.S. Jessen, *Phys. Rev. Lett.* **74**, 1542 (1995).

[50] C. Ekstrom, E. Burt, T Swanson, 2000 Proc. 14$^{\text{th}}$ Eur. Frequency and Time Forum, p. 502.

[51] S. Weyers, A. Bauch, U. Huebner, R. Schroeder, C. Tamm, *IEEE Trans. Ultrason. Ferroelectr. Freq. Control.* **47**, 432 (2000).

[52] P. Treutlein, K. Yeow Chung, S. Chu, *Phys. Rev.* **A63**, 051401, (2001).

[53] A. Kerman, V. Vuletic, C. Chin, S. Chu, *Phys. Rev. Lett.* **84**, 439 (2000).

[54] P. Lemonde *et al.*, *Frequency Measurement and Control — Advanced Techniques and Future Trends*, Springer, Berlin 2001, p. 131.

[55] S. Ohshima, *Proc. 5th Symp. on Freqency Standards and Metrology*, World Scientific, Singapore 1995, p. 60.

[56] F. Levi, A. Godone, L. Lorini, *Proc. 6th Symp. on Freqency Standards and Metrology*, World Scientific, Singapore, to be published.

[57] R. Legere, K. Gibble, *Phys. Rev. Lett.* **81**, 5780 (1998).

[58] G. Dudle, G. Mileti, A. Joyet, E. Fretel, P. Berthoud, P. Thomann, *IEEE Transactions on Ultrasonics Ferroelectrics and Frequency Control*, **UFFC-47**, 438 (2000).

[59] C. Fertig, K. Gibble, *Phys Rev. Lett.* **85**, 1622 (2000).

[60] Y. Sortais, S. Bize, C. Nicolas, A. Clairon, C. Salomon, C. Williams, *Phys. Rev. Lett.* **85**, 3117, (2000).

[61] S. Diddams, D. Jones, J. Ye, S. Cundiff, J. Hall, J. Ranka, R. Windeler, R. Holzwarth, T. Udem, T. Hänsch, *Phys. Rev. Lett.* **84**, 5102 (2000).

[62] T. Heavner, *Proc. 6th Symp. on Freqency Standards and Metrology*, World Scientific, Singapore, to be published.

[63] T.E. Parker, P. Hetzel, S.R. Jefferts, S. Weyers, L.M. Nelson, A. Bauch, J. Levine, Proc. 2001 IEEE Int. Frequency Control Symposium.

[64] M. Niering, R. Holzwarth, J. Reichert, P. Pokasov, T. Udem, M. Weitz, T. Hänsch P. Lemonde, G. Santarelli, M. Abgrall, P. Laurent, C. Salomon, A. Clairon, *Phys. Rev. Lett.* **84**, 5496 (2000).

[65] T.J. Quinn, *Metrologia* **36**, 211 (1999).

[66] J. Reichert, M. Niering, R. Holzwarth, M. Weitz, T. Udem, T.W. Haensch, *Phys. Rev. Lett.* **84**, 3232 (2000).

[67] J.L. Hall, M. Zhu, P. Buch, *J. Opt. Soc. Am.* **B6**, 2194 (1989).

[68] H. Wallis, W. Ertmer, *J. Opt. Soc. Am.* **B6**, 2211 (1989).

[69] F. Riehle, H. Schnatz, B. Lipphardt, G. Zinner, T. Trebst, J. Helmke, *IEEE Trans. Instrum. Meas.* **48**, 613 (1999).

[70] L. Hollberg *et al., IEEE J. Quant. Electron.* **37**, 1502 (2001).

[71] C.J. Bordé, C. Salomon, S. Avrillier, A. Van Lerberghe, C. Bréant, D. Bassi, G. Scoles, *Phys. Rev.* **A30**, 1836 (1984).

[72] V. Vassiliev, V. Velichansky, P. Kersten, T. Trebst, F. Riehle, *Opt. Lett.* **23**, 1229 (1998).

[73] C.W. Oates, E.A. Curtis, L. Hollberg, *Opt. Lett.* **25**, 1603 (2000).

[74] K.R. Vogel, T.P. Dinneen, A. Gallagher, J.L. Hall, *IEEE Trans. Instrum. Meas.* **48**, 618 (1999).

[75] H. Katori, T. Ido, Y. Isoya, M. Kuwata-Gonokami, *Phys. Rev. Lett.* **82**, 1116 (1999).

[76] T. Ido, Y. Isoya, H. Katori, *Phys. Rev.* **A61**, 061403 (2000).

[77] G. Uhlenberg, J. Dirscherl, H. Walther, *Phys. Rev.* **A62**, 063404 (2000).

[78] T. Badr, S. Guérandel, M. Plimmer, P. Juncar, M.E. Himbert, *Eur. Phys. J.* **D14**, 39 (2001).

[79] For a review of ion trapping techniques, see R. Blatt, P. Gill, R.C. Thompson, *J. Mod. Opt.* **39**, 193 (1992).

[80] H. Dehmelt, *IEEE Trans. Instrum. Meas.* **31**, 83 (1982).

[81] J.E. Bernard, A.A. Madej, L. Marmet, B.G. Whitford, K.J. Siemsen, S. Cundy, *Phys. Rev. Lett.* **82**, 3228 (1999).

[82] G.P. Barwood, K. Gao, P. Gill, G. Huang, H.A. Klein, *IEEE Trans. Instrum. Meas.* **50**, 543 (2001).

[83] G.P. Barwood, K. Gao, P. Gill, G. Huang, H.A. Klein, *SPIE Proc.* **4269**, 134 (2001); G.P. Barwood, G. Huang, H.A. Klein, P. Gill, R.B.M. Clarke, *Phys. Rev.* **A59**, 3178 (1999).

[84] M.G. Boshier, G.P. Barwood, G. Huang, H.A. Klein, *Appl. Phys.* **B71**, 51 (2000).

[85] G. Werth, *Metrologia* **22**, 190 (1986).

[86] M. Roberts, P. Taylor, S.V. Gateva-Kostova, R.B.M. Clarke, W.R.C. Rowley, P. Gill, *Phys. Rev.* **A60**, 2867 (1999).

[87] C. Tamm, D. Engelke, V. Buehner, *Phys. Rev.* **A61**, 053405 (2000).

[88] M. Roberts, P. Taylor, G.P. Barwood, W.R.C. Rowley, P. Gill, *Phys. Rev.* **A62**, 020501 (2000).

[89] S.A. Webster, P. Taylor, M. Roberts, G.P. Barwood, P. Gill, *Phys. Rev.* **A65**, 052501 (2002).

[90] B.C. Young, F.C. Cruz, W.M. Itano, J.C. Bergquist, *Phys. Rev. Lett.* **82**, 3799 (1999).

[91] R.J. Rafac, B.C. Young, J.A. Beall, W.M. Itano, D.J. Wineland, J.C. Bergquist, *Phys. Rev. Lett.* **85**, 2462 (2000).

[92] H. Dehmelt, *Bull. Am. Phys. Soc.* **18**, 1521 (1973).

[93] W. Nagourney, E. Burt, H.G. Dehmelt, in *Proceedings of the Fifth Symposium on Frequency Standards and Metrology*, ed. J.C. Bergquist, World Scientific, Singapore 1996, p. 341.

[94] T. Becker, J. von Zanthier, A.Y. Nevsky, C. Schwedes, M.N. Skvortsov, H. Walther, E. Peik, *Phys. Rev. Lett.* **63**, 051802 (2001).

[95] H. Schnatz, B. Lipphardt, J. Helmcke, F. Riehle, G. Zinner, *Phys. Rev. Lett.* **76**, 18 (1996).

[96] J.N. Eckstein, A.I. Ferguson, T.W. Haensch, *Phys. Rev. Lett.* **40**, 847 (1978).

[97] D.E. Spence, P.N. Kean, W. Sibbett, *Opt. Lett.* **16**, 42 (1991).

[98] T. Udem *et al., Phys. Rev. Lett.* **82**, 3568 (1999).

[99] J.C. Knight, T.A. Birks, P. St J. Russell, D.M. Atkins, *Opt. Lett.* **21**, 1547 (1996).

[100] J.K. Ranka, R.S. Windeler, A.J. Stentz, *Opt. Lett.* **25**, 25 (2000).

[101] D. Jones *et al., Science* **288**, 635 (2000).

[102] R. Holzwarth *et al., Phys. Rev. Lett.* **85**, 2264 (2000).

[103] T. Udem *et al., Phys. Rev. Lett.* **86**, 4996 (2001).

[104] J. Stenger, C. Tamm, N. Haverkamp, S. Weyers, H.R. Telle, *Opt. Lett.* **26**, 1589 (2001).

[105] J. Stenger *et al., Phys. Rev.* **A63**, 021802 (2001).

[106] S.N. Lea *et al.,* in *Proceedings of the Sixth Symposium on Frequency Standards and Metrology*, ed. P. Gill, World Scientific, Singapore 2002, p. 144.

[107] S.A. Diddams, L. Hollberg, L.-S. Ma, L. Robertsson, *Opt. Lett.* **27**, 58 (2002).

[108] S.A. Diddams *et al., Science* **293**, 825 (2001).